


Twins Percolation for Qubit Losses in Topological Color Codes

Davide Vodola,¹ David Amaro,¹ Miguel Angel Martin-Delgado,² and Markus Müller¹
¹*Department of Physics, Swansea University, Singleton Park, Swansea SA2 8PP, United Kingdom*
²*Departamento de Física Teórica I, Universidad Complutense, 28040 Madrid, Spain*

 (Received 7 March 2018; published 6 August 2018)

In this Letter, we establish and explore a new connection between quantum information theory and classical statistical mechanics by studying the problem of qubit losses in 2D topological color codes. We introduce a protocol to cope with qubit losses, which is based on the identification and removal of a twin qubit from the code, and which guarantees the recovery of a valid three-colorable and trivalent reconstructed color code. Moreover, we show that determining the corresponding qubit loss error threshold is equivalent to a new generalized classical percolation problem. We numerically compute the associated qubit loss thresholds for two families of 2D color code and find that with $p = 0.461 \pm 0.005$ these are close to satisfying the fundamental limit of 50% as imposed by the no-cloning theorem. Our findings reveal a new connection between topological color codes and percolation theory, show high robustness of color codes against qubit loss, and are directly relevant for implementations of topological quantum error correction in various physical platforms.

DOI: [10.1103/PhysRevLett.121.060501](https://doi.org/10.1103/PhysRevLett.121.060501)

Quantum information theory, widely recognized as a powerful paradigm to formulate and address problems in information processing beyond the realms of classical physics, has shown strong cross connections to different fields, including atomic, molecular and optical (AMO) physics [1], condensed matter [2,3], computer science [4], but also classical statistical mechanics. Exploring the connection between quantum information and classical statistical physics has proven particularly fruitful in both directions and revealed deep and unexpected links. For instance, efficient quantum algorithms enable estimating partition functions of classical spin systems [5–14]. In the context of fault-tolerant quantum computing, topological quantum error correcting (QEC) codes, such as Kitaev’s surface code [15,16] and color codes [17,18], protect quantum information in two- or higher-dimensional lattices of qubits. They provide to date, arguably, the most promising route towards practical fault-tolerant quantum computers [19]. Here, the problem of studying the error robustness of these topological quantum codes can be mapped onto classical statistical mechanics lattice models [16], opening a powerful avenue to study fundamental features of the corresponding QEC codes.

For instance, error thresholds and the parameter regimes where QEC succeeds (fails) are identified with the critical point and ordered (disordered) phases of the classical models, respectively. Depending on the quantum code and error model considered, different classical models emerge: For computational errors only, such as uncorrelated bit and phase flips, QEC can be mapped to a classical 2D random-bond Ising model with two-body interactions for the toric code [16] and three-body interactions for the

color code [20]. If measurements in the QEC procedure are also faulty, the QEC problem maps for the toric code onto a classical 3D random plaquette gauge model [16,21] and for color codes onto a 3D lattice gauge theory, introduced for the first time in Ref. [22].

Qubit loss, caused by actual loss of particles or photons, or by leakage processes that take the qubit out of the computational space, is an additional severe error source in many physical platforms, with some counterstrategies developed [23–28]. For the surface code affected by qubit losses, correction of losses is related to a classical bond percolation transition on a square lattice [29–32]. For topological color codes, on the contrary, to date it is an open question (i) how to cope with qubit losses, (ii) if and to what classical model the problem of qubit loss correction can be mapped, and (iii) what level of robustness against losses color codes offer.

In this Letter, we address the problem of qubit losses in topological color codes by (i) introducing an explicit novel protocol (algorithm) to correct detectable and locatable losses, (ii) establishing a mapping of QEC color codes affected by losses onto a novel model of classical percolation and (iii) exploiting this mapping to compute the fundamental qubit loss error threshold in color codes associated with our protocol. Our results establish a new connection with classical percolation, and they are also directly relevant for practical QEC with trapped ions [33–37], Rydberg atoms [38–40], photons [41,42], and superconductors [43–46].

The color code [17] is a topological QEC code defined by a stabilizer group \mathcal{S} acting on physical qubits placed at the vertices of a trivalent, three-colorable 2D lattice [see

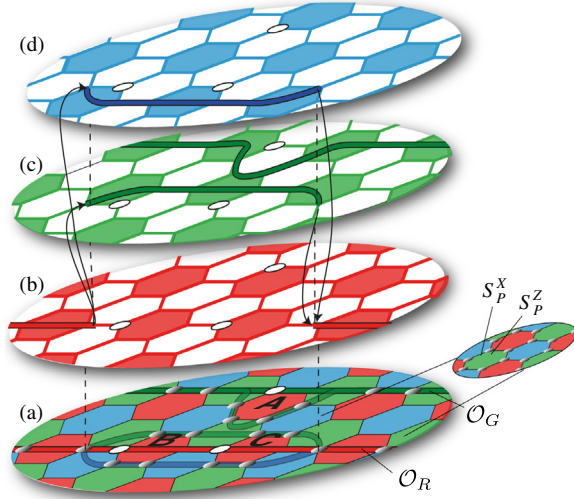


FIG. 1. (a) Excerpt of a hexagonal 2D color code. Physical qubits reside at the vertices of the lattice, and each plaquette P hosts an X and Z -type generator S_P^X, S_P^Z of the stabilizer group of the code. Logical (string) operators \mathcal{O}_G and \mathcal{O}_R can be deformed by stabilizers, to evade qubit loss locations (white circles): for example, \mathcal{O}_G is deformed by the generator A into the lighter green path, whereas the red string \mathcal{O}_R branches into an equivalent green and blue string by the action of generators B and C . For clarity, only qubits on which \mathcal{O}_G and \mathcal{O}_R have support are shown. Note that the branched red operator belongs to all three shrunk lattices of plaquettes as shown in panels (b),(c),(d).

Fig. 1(a)]. Each plaquette P has an even number of vertices and hosts two types of mutually commuting generators of \mathcal{S} , defined as $S_P^\sigma = \prod_{j \in P} \sigma_j$, where σ is a Pauli X or Z operator acting on all qubits j belonging to P . As the lattice is three-colorable, one can associate one color c (among R, G, B) to each plaquette and hence to each generator such that if two plaquettes share an edge they will be of different color. Each plaquette will also belong to one shrunk colored sublattice like in Figs. 1(b)–1(d) [47]. The code space \mathcal{C} , i.e., the Hilbert subspace hosting logical states, is the simultaneous $+1$ eigenstate of all S_P^σ stabilizers. The number of logical qubits k depends on the topology of the manifold in which the system is embedded: for a surface of Euler characteristic χ one finds $k = 4 - 2\chi$ [17]. The definition of the logical operators, T_μ^σ , for $\mu = 1, \dots, k$ and $\sigma = X, Z$, also depends on the topology; e.g., for a torus they are associated with the two nontrivial cycles around it [47,52].

The protocol for losses.—The scheme to correct losses that we propose and analyze here requires (i) detecting the lost qubits, (ii) redefining the set of stabilizer generators such that each of them has support only on qubits not affected by loss, (iii) checking if the encoded logical quantum states are unaffected by the losses, and (iv) finally removing possible excitations (-1 eigenstates of newly defined stabilizer generators). We remark that our protocol works for detectable and locatable losses; i.e., it requires

TABLE I. Pseudocode summarizing the loss recovery protocol.

(i) <i>Input:</i> \mathcal{Q} = list of detected lost qubits	
(ii) <i>Output:</i> Valid color code	
For q_0 in \mathcal{Q} do	
$\mathcal{L}_0 \leftarrow \{\ell_1, \ell_2, \ell_3\}$	[links from q_0]
$c_j \leftarrow$ color of link ℓ_j	
$q_j \leftarrow$ neighbor of q_0 via ℓ_j	
$q_1 \leftarrow$ twin qubit randomly chosen	
$\mathcal{L}_1 \leftarrow \{m_2, m_3\}$	[links from q_1]
$s_j \leftarrow$ qubit connected to q_1 via m_j	
Remove $q_0, q_1, \mathcal{L}_0, \mathcal{L}_1$	
Connect q_j, s_j by a link of color c_j	
(iii) Check existence of logical operator	
(iv) Remove excitations	

the positions of lost qubits \mathcal{Q} to be determined up front [53–55]. Assuming that \mathcal{Q} is known (i), we will now focus on the key steps (ii)–(iii) of the protocol and refer for details on (iv) to the Supplemental Material [47].

Redefinition of stabilizers.—For color codes one main challenge is (ii) to redefine a modified set of stabilizers respecting the constraint that the resulting modified lattice hosting the color code remains three-colorable and trivalent. The protocol we propose to achieve this is summarized in Table I: (1) given a detected lost qubit q_0 [white circle in Figs. 2(a) and 2(b)] we choose randomly a *twin qubit* q_1 among its three neighboring qubits. This twin qubit will be *sacrificed*, i.e., also removed from the code [Fig. 2(c)]. We refer to the pair of qubits q_0 and q_1 and the link connecting them as a *dimer*. Note that the dimer connects two plaquettes of the same color [plaquettes 1 and 4 in Fig. 2(b)], it is shared by two neighboring plaquettes of the two complementary colors [plaquettes 2 and 3 in Fig. 2(b)] and it is connected to four links ℓ_2, ℓ_3, m_2, m_3 (one pair for each of the complementary two colors), see dashed lines in Fig. 2(c). (2) The dimer, as well as the four links originating from it are removed. Then, to redefine a valid trivalent and three-colorable lattice, the two pairs of qubits with links of the same colors as the removed ones are connected by new links [Fig. 2(c)]. Thereby, the two plaquettes originally connected by the dimer will merge into a single larger plaquette, whereas the two plaquettes that were sharing the dimer will shrink, with their qubit number being reduced by two [Fig. 2(d)]. This ensures that the number of vertices on all reconstructed plaquettes remains even. Steps (1) and (2) are repeated iteratively for all losses. The final lattice is guaranteed to be trivalent and three colorable, see Fig. 2(e) for an example. The validity of our protocol can be substantiated by computing the Euler characteristic of the resulting lattice. Before the occurrence of a loss, $\chi = V - E + F$ where $V, E,$ and F denote the numbers of qubits, links, and plaquettes of the lattice. After (1) and (2), χ remains unchanged, as $\chi' = (V - 2) - (E - 3) + (F - 1) = \chi$, and so does, consequently, the number of logical qubits.

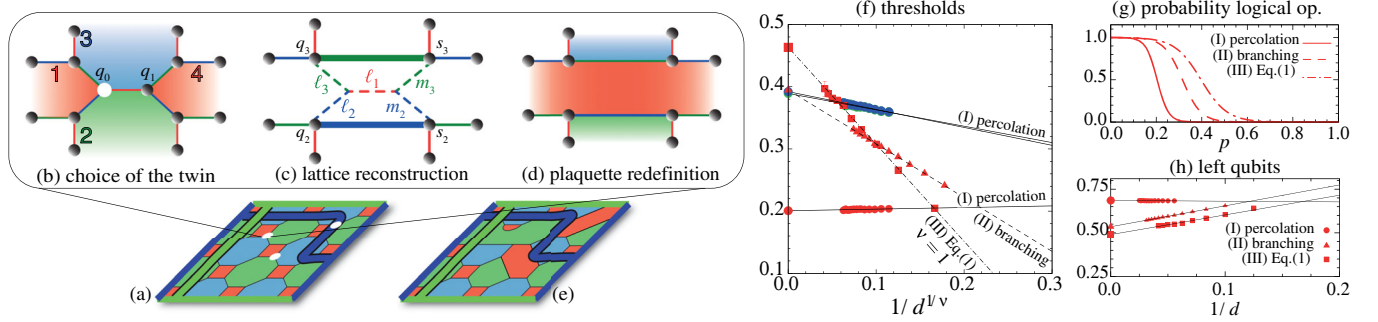


FIG. 2. (a) Representation of a distance $d = 6$ color code, on a 4.8.8 lattice, affected by three qubit losses (white circles). This code stores two logical qubits, with four logical operators defined along green and blue strings that connect opposite borders of the corresponding colors. Panels (b)–(d): Loss recovery protocol (see also main text). (b) Twin identification. (c) Link removal and lattice reconstruction. (d) Plaquette redefinition. (e) Reconstructed lattice after loss correction. A logical operator (e.g., the blue one) potentially affected by a loss can be transformed into an equivalent one by multiplication with a stabilizer. (f) Loss thresholds for a 4.8.8 lattice computed by checking percolation for the three logical operators (filled circles), branching (filled triangle) and the existence of solutions of Eq. (1) (filled square) only for the red logical operator. Thresholds are plotted as a function of $1/d^{1/\nu}$, with d the logical distance and $\nu = 4/3$ for the methods (I,II) while $\nu = 1$ for the method (III). The intercepts of the black lines (marked with the same symbols as the data) represent the critical threshold for $d \rightarrow \infty$. (g) Probability to find a logical red operator using the methods (I,II,III) as a function of the loss rate p for a 4.8.8 lattice of distance $d = 36$. (h) Fraction of qubits left in the lattice for each of the three methods as a function of $1/d$. For methods (II) and (III), the fractions approach the fundamental 50% limit.

Check of the existence of the logical operators.—In order to understand whether or not a given set of losses affects the logical quantum information, one has to verify whether the logical operators remain intact. The support of logical operators is not unique [47]; thus one can obtain equivalent logical operators \tilde{T}_μ^σ by multiplying an original one, T_μ^σ , by any element of \mathcal{S} . This equivalence can be used to check if a logical operator is still defined by considering that it is possible to recover the μ th logical qubit if one can find a subset $\mathcal{V} \subseteq \mathcal{S}$, such that the modified logical operators

$$\tilde{T}_\mu^\sigma = T_\mu^\sigma \prod_{S_p^\sigma \in \mathcal{V}} S_p^\sigma \quad (1)$$

have vanishing support on lost and twin qubits. If that is not possible, T_μ^σ is in an undefined state and the encoded quantum information is corrupted.

We consider three ways of checking if logical operators remain unaffected by the losses and code reconstruction:

(I) The first one uses the fact that logical operators can take the form of nontrivial colored strings spanning the entire lattice like, e.g., the green logical operator \mathcal{O}_G in Fig. 1(a). If \mathcal{O}_G is multiplied by the stabilizer of the red plaquette A, it is deformed into the string operator with support on the lighter green path, but it still belongs to the green shrunk lattice [Fig. 1(c)]. Thus, the question is whether one can find *percolating strings* in the shrunk lattices without support on losses and twin qubits. This is equivalent to finding a logical operator \tilde{T}_μ^σ as a solution of Eq. (1) under the constraint of choosing elements of the subset \mathcal{V} of the original \mathcal{S} only among the stabilizers of the two colors that are complementary to the color of T_μ^σ . Note that since one uses the original group \mathcal{S} to find equivalent

logical operators, these strings have support on chains made up by links which belong to the original lattice.

(II) The second way is by considering that the subset \mathcal{V} can be formed also by stabilizers of the same color as T_μ^σ . If, e.g., a red logical operator \mathcal{O}_R [Fig. 1(a)] is multiplied by stabilizers of two red plaquettes B and C, it will split into a green and blue string [Figs. 1(b)–1(d)]. This string branching, not present in surface codes [15,16], is peculiar to color codes, allowing logical operators to take the form of string nets [17]. The existence check is then translated into a combined percolation check in the coupled three shrunk lattices. For, say, the operator \mathcal{O}_R , the starting point of such branching [Fig. 1(b)] is a qubit that has a red link where a loss or a twin qubit resides and the green and the blue unaffected links both belong to the original lattice. Then, the red operator can split up and percolate as a blue and a green string into the two shrunk lattices [Figs. 1(c) and 1(d)]. The ending point of the branching is required to be a qubit having all the three unaffected links belonging to the original lattice. Thereby, the blue and green strings eventually recombine into the red one that continues its way in the red shrunk lattice.

(III) The third way consists in efficiently solving Eq. (1) directly [47], allowing for multiplication of logical operators with elements from the whole original stabilizer group. This method defines the *fundamental limit* p_{fund} for the code as it captures the most general admissible forms of logical operators corresponding to percolating string nets with, in general, several branching and fusing points at which the three coupled shrunk lattices supporting the string net are coupled.

The two methods (II) and (III) are a generalized percolation problem that effectively deforms the operator

by branching it into all three shrunk lattices. It is instructive to contrast our protocol for color codes with the pioneering protocol for qubit losses in the surface code [29]. There, two neighbouring plaquettes affected by a loss on the shared link can be fused into one larger plaquette (see Ref. [47]) that hosts one new stabilizer without support on the lost qubit. Logical operators remain string-type and can be deformed so they evade the link corresponding to the lost qubit. Thus, the qubit loss problem in the surface code maps onto the bond-percolation problem on a 2D square lattice with associated threshold of $1/2$ [48].

Numerical results.—To study the robustness against losses, using the above protocol, we consider 2D color codes of different logical distances d defined on planar 4.8.8 and a 6.6.6 lattices [47]. For each of the distances d , we generate random sequences of losses by Monte Carlo simulations, then reconstruct the lattice according to our protocol, and finally check (I) if percolating strings exist, (II) if percolating branched strings exist and (III) if the linear system of Eqs. (1) admits solutions. For a fixed distance d , these checks provide the critical thresholds $p(d)$, i.e., the fraction of losses at which the logical operators can no longer be defined.

For the existence check of percolating strings (I) in a code of distance d , we compute, for each of the three colored shrunk lattices, the critical fraction $p(d)$ at which a percolating string-type path ceases to exist. Percolation theory [48] predicts the critical fraction $p(d)$ to scale in the limit $d \rightarrow \infty$ as $p(d) - p_\infty \propto 1/d^{1/\nu}$ with a scaling exponent ν . Numerically we find $\nu = 4/3$, which is the value expected from percolation theory [48]. Figure 2(f) shows $p(d)$ and least-square linear fits whose intercepts for $1/d^{1/\nu} \rightarrow 0$ yield the string percolation thresholds p_{perc} for each of the string-type logical operators of the three different colors. We obtain similar results for the 6.6.6 lattice [47]. Red string-type logical operators have a lower threshold as the structure of the supporting red shrunk lattice is different from the other two ones. However, if we allow for (II) string branching, i.e., the red logical operator can split up into a green and a blue path [as in Fig. 1(a)], and we compute, for $d \rightarrow \infty$, the fraction p_{branch} at which a logical operator ceases to exist on the reconstructed coupled three shrunk lattices, we obtain a value compatible with p_{perc} for the green and blue operators [red triangles along the dashed line in Fig. 2(f)]. This result indicates that at a loss rate for which a red string-type operator no longer percolates, branching allows the logical operator to evade the nonpercolating red shrunk lattice and percolate on the green and blue lattices instead, thereby almost doubling its robustness, from $p_{\text{perc}} \approx 0.2$ to 0.4 . Finally, we apply method (III) that checks the existence of a solution to Eq. (1). As expected, this yields the highest threshold of $p_{\text{fund}} = (0.461 \pm 0.005)$ [Fig. 2(f), dot dashed line, linear fit of the data with $\nu = 1$]. Figure 2(g) displays the probability of finding a red logical operator as obtained

from the three methods (I–III) for a $d = 36$ lattice. The curves mark the boundary separating regions, where the logical qubit associated to a logical operator can and cannot be recovered.

A natural question is how many qubits are left in the lattice at the percolation threshold, beyond which the encoded logical information cannot be fully restored. For our protocol, for low loss rates $p \ll 1$, when losses are sparsely distributed over the lattice, the fraction of remaining qubits is given by $1 - 2p$ as for each loss one twin qubit is also removed. However, for larger p the sets of losses and of twin qubits can have a nonempty intersection, as, e.g., one of the twin qubits could correspond also to a loss. Figure 2(h) shows the fraction of qubits left in the lattice for each of the three methods (I–III) as a function of $1/d$. Notably, when considering methods (II) and (III), this number approaches 50%, which is the fundamental limit as imposed by the no-cloning theorem for the capacity of a quantum erasure channel [56]. This shows the high intrinsic loss robustness of color codes and also underlines the near optimality of our recovery protocol based on a purely *local* reconstruction, not taking into account the *global* configuration of losses.

Conclusions and outlook.—In this Letter, we have introduced an operationally defined and efficient protocol to cope with qubit losses in color codes, which preserves the three colorability of the resulting reconstructed 2D lattice. We have established a new mapping of QEC color codes affected by qubit loss onto a novel model of classical percolation on coupled lattices. Finally, we have shown that color codes in combination with our qubit loss correction protocol are highly robust against losses, almost saturating the fundamental limit set by the no-cloning theorem. The protocol discussed can be extended to also account for computational and measurement errors, similar to studies for the surface code in which a robustness trade-off between the error thresholds for both error sources was found [29,31]. Furthermore, we hope that the cross connection of the QEC problem with a new generalised percolation problem will stimulate further research that leverages tools and results from percolation theory to investigate the robustness of other topological QEC codes and many-body quantum phases of matter under loss of particles.

D. V. thanks M. Gutiérrez for fruitful discussions. We acknowledge support by U.S. A.R.O. through Grant No. W911NF-14-1-010. The research is also based upon work supported by the Office of the Director of National Intelligence (ODNI), Intelligence Advanced Research Projects Activity (IARPA), via the U.S. Army Research Office Grant No. W911NF-16-1-0070. M. A. M. D. acknowledges support from Spanish MINECO Grant No. FIS2015-67411, and the CAM research consortium QITEMAD+, Grant No. S2013/ICE-2801. We acknowledge the resources and support of High Performance

Computing Wales, where most of the simulations were performed, as well as the HPC-Université de Strasbourg. The views and conclusions contained herein are those of the authors and should not be interpreted as necessarily representing the official policies or endorsements, either expressed or implied, of the ODNI, IARPA, or the U.S. Government. The U.S. Government is authorized to reproduce and distribute reprints for Governmental purposes notwithstanding any copyright annotation thereon. Any opinions, findings, and conclusions or recommendations expressed in this material are those of the author(s) and do not necessarily reflect the view of the U.S. Army Research Office.

-
- [1] T. D. Ladd, F. Jelezko, R. Laflamme, Y. Nakamura, C. Monroe, and J. L. O'Brien, Quantum computers, *Nature (London)* **464**, 45 (2010).
- [2] M. Lewenstein, A. Sanpera, V. Ahufinger, B. Damski, A. Sen(De), and U. Sen, Ultracold atomic gases in optical lattices: mimicking condensed matter physics and beyond, *Adv. Phys.* **56**, 243 (2007).
- [3] L. Amico, R. Fazio, A. Osterloh, and V. Vedral, Entanglement in many-body systems, *Rev. Mod. Phys.* **80**, 517 (2008).
- [4] M. A. Nielsen and I. L. Chuang, *Quantum Computation and Quantum Information* (Cambridge University Press, Cambridge, England, 2000).
- [5] D. A. Lidar and O. Biham, Simulating Ising spin glasses on a quantum computer, *Phys. Rev. E* **56**, 3661 (1997).
- [6] R. D. Somma, C. D. Batista, and G. Ortiz, Quantum Approach to Classical Statistical Mechanics, *Phys. Rev. Lett.* **99**, 030603 (2007).
- [7] M. Van den Nest, W. Dür, and H. J. Briegel, Classical Spin Models and the Quantum-Stabilizer Formalism, *Phys. Rev. Lett.* **98**, 117207 (2007).
- [8] J. Geraci and D. A. Lidar, On the exact evaluation of certain instances of the Potts partition function by quantum computers, *Commun. Math. Phys.* **279**, 735 (2008).
- [9] G. De las Cuevas, W. Dür, H. J. Briegel, and M. A. Martin-Delgado, Unifying All Classical Spin Models in a Lattice Gauge Theory, *Phys. Rev. Lett.* **102**, 230502 (2009).
- [10] J. Geraci and D. A. Lidar, Classical Ising model test for quantum circuits, *New J. Phys.* **12**, 075026 (2010).
- [11] G. D. las Cuevas, W. Dür, M. V. den Nest, and M. A. Martin-Delgado, Quantum algorithms for classical lattice models, *New J. Phys.* **13**, 093021 (2011).
- [12] Y. Xu, G. D. las Cuevas, W. Dür, H. J. Briegel, and M. A. Martin-Delgado, The $U(1)$ lattice gauge theory universally connects all classical models with continuous variables, including background gravity, *J. Stat. Mech.* (2011) P02013.
- [13] G. De las Cuevas and T. S. Cubitt, Simple universal models capture all classical spin physics, *Science* **351**, 1180 (2016).
- [14] M. H. Zarei and A. Montakhab, Dual correspondence between classical spin models and quantum CSS states, [arXiv:1710.01902](https://arxiv.org/abs/1710.01902).
- [15] A. Kitaev, Fault-tolerant quantum computation by anyons, *Ann. Phys. (Amsterdam)* **303**, 2 (2003).
- [16] E. Dennis, A. Kitaev, A. Landahl, and J. Preskill, Topological quantum memory, *J. Math. Phys. (N.Y.)* **43**, 4452 (2002).
- [17] H. Bombin and M. A. Martin-Delgado, Topological Quantum Distillation, *Phys. Rev. Lett.* **97**, 180501 (2006).
- [18] H. Bombin and M. A. Martin-Delgado, Topological Computation without Braiding, *Phys. Rev. Lett.* **98**, 160502 (2007).
- [19] B. M. Terhal, Quantum error correction for quantum memories, *Rev. Mod. Phys.* **87**, 307 (2015).
- [20] H. G. Katzgraber, H. Bombin, and M. A. Martin-Delgado, Error Threshold for Color Codes and Random Three-Body Ising Models, *Phys. Rev. Lett.* **103**, 090501 (2009).
- [21] T. Ohno, G. Arakawa, I. Ichinose, and T. Matsui, Phase structure of the random-plaquette Z_2 gauge model: accuracy threshold for a toric quantum memory, *Nucl. Phys.* **B697**, 462 (2004).
- [22] R. S. Andrist, H. G. Katzgraber, H. Bombin, and M. A. Martin-Delgado, Tricolored lattice gauge theory with randomness: Fault tolerance in topological color codes, *New J. Phys.* **13**, 083006 (2011).
- [23] M. Grassl, T. Beth, and T. Pellizzari, Codes for the quantum erasure channel, *Phys. Rev. A* **56**, 33 (1997).
- [24] T. C. Ralph, A. J. F. Hayes, and A. Gilchrist, Loss-Tolerant Optical Qubits, *Phys. Rev. Lett.* **95**, 100501 (2005).
- [25] C.-Y. Lu, W.-B. Gao, J. Zhang, X.-Q. Zhou, T. Yang, and J.-W. Pan, Experimental quantum coding against qubit loss error, *Proc. Natl. Acad. Sci. U.S.A.* **105**, 11050 (2008).
- [26] J. A. Sherman, M. J. Curtis, D. J. Szwer, D. T. C. Allcock, G. Imreh, D. M. Lucas, and A. M. Steane, Experimental Recovery of a Qubit from Partial Collapse, *Phys. Rev. Lett.* **111**, 180501 (2013).
- [27] S. Mehl, H. Bluhm, and D. P. DiVincenzo, Fault-tolerant quantum computation for singlet-triplet qubits with leakage errors, *Phys. Rev. B* **91**, 085419 (2015).
- [28] J. Ghosh and A. G. Fowler, Leakage-resilient approach to fault-tolerant quantum computing with superconducting elements, *Phys. Rev. A* **91**, 020302 (2015).
- [29] T. M. Stace, S. D. Barrett, and A. C. Doherty, Thresholds for Topological Codes in the Presence of Loss, *Phys. Rev. Lett.* **102**, 200501 (2009).
- [30] T. M. Stace and S. D. Barrett, Error correction and degeneracy in surface codes suering loss, *Phys. Rev. A* **81**, 022317 (2010).
- [31] M. Ohzeki, Error threshold estimates for surface code with loss of qubits, *Phys. Rev. A* **85**, 060301 (2012).
- [32] S. Nagayama, A. G. Fowler, D. Horsman, S. J. Devitt, and R. V. Meter, Surface code error correction on a defective lattice, *New J. Phys.* **19**, 023050 (2017).
- [33] J. Chiaverini, D. Leibfried, T. Schaetz, M. D. Barrett, R. B. Blakestad, J. Britton, W. M. Itano, J. D. Jost, E. Knill, C. Langer, R. Ozeri, and D. J. Wineland, Realization of quantum error correction, *Nature (London)* **432**, 602 (2004).
- [34] P. Schindler, J. T. Barreiro, T. Monz, V. Nebendahl, D. Nigg, M. Chwalla, M. Hennrich, and R. Blatt, Experimental repetitive quantum error correction, *Science* **332**, 1059 (2011).
- [35] B. P. Lanyon, P. Jurcevic, M. Zwerger, C. Hempel, E. A. Martinez, W. Dür, H. J. Briegel, R. Blatt, and C. F. Roos, Measurement-Based Quantum Computation with Trapped Ions, *Phys. Rev. Lett.* **111**, 210501 (2013).

- [36] D. Nigg, M. Müller, E. A. Martinez, P. Schindler, M. Hennrich, T. Monz, M. A. Martin-Delgado, and R. Blatt, Quantum computations on a topologically encoded qubit, *Science* **345**, 302 (2014).
- [37] J. G. Bohnet, B. C. Sawyer, J. W. Britton, M. L. Wall, A. M. Rey, M. Foss-Feig, and J. J. Bollinger, Quantum spin dynamics and entanglement generation with hundreds of trapped ions, *Science* **352**, 1297 (2016).
- [38] L. Isenhower, E. Urban, X. L. Zhang, A. T. Gill, T. Henage, T. A. Johnson, T. G. Walker, and M. Saffman, Demonstration of a Neutral Atom Controlled-NOT Quantum Gate, *Phys. Rev. Lett.* **104**, 010503 (2010).
- [39] T. Wilk, A. Gaëtan, C. Evellin, J. Wolters, Y. Miroshnychenko, P. Grangier, and A. Browaeys, Entanglement of Two Individual Neutral Atoms using Rydberg Blockade, *Phys. Rev. Lett.* **104**, 010502 (2010).
- [40] M. Saffman, T. G. Walker, and K. Mølmer, Quantum information with Rydberg atoms, *Rev. Mod. Phys.* **82**, 2313 (2010).
- [41] J. L. O'Brien, G. J. Pryde, A. G. White, and T. C. Ralph, High-fidelity z -measurement error encoding of optical qubits, *Phys. Rev. A* **71**, 060303 (2005).
- [42] T. B. Pittman, B. C. Jacobs, and J. D. Franson, Demonstration of quantum error correction using linear optics, *Phys. Rev. A* **71**, 052332 (2005).
- [43] R. Barends *et al.*, Superconducting quantum circuits at the surface code threshold for fault tolerance, *Nature (London)* **508**, 500 (2014).
- [44] J. Kelly *et al.*, State preservation by repetitive error detection in a superconducting quantum circuit, *Nature (London)* **519**, 66 (2015).
- [45] A. D. Córcoles, E. Magesan, S. J. Srinivasan, A. W. Cross, M. Steffen, J. M. Gambetta, and J. M. Chow, Demonstration of a quantum error detection code using a square lattice of four superconducting qubits, *Nat. Commun.* **6**, 6979 (2015).
- [46] N. Ofek, A. Petrenko, R. Heeres, P. Reinhold, Z. Leghtas, B. Vlastakis, Y. Liu, L. Frunzio, S. M. Girvin, L. Jiang, M. Mirrahimi, M. H. Devoret, and R. J. Schoelkopf, Extending the lifetime of a quantum bit with error correction in superconducting circuits, *Nature (London)* **536**, 441 (2016).
- [47] See Supplemental Material at <http://link.aps.org/supplemental/10.1103/PhysRevLett.121.060501> for a discussion on (i) the lattice geometries we studied numerically, (ii) the methods we used to find equivalent logical operators, (iii) the protocol for correcting from losses in Kitaev's code, (iv) the removal of excitations in the modified stabilizer group, (v) some additional results for the 6.6.6 and the triangular lattices. The Supplemental Material includes Refs. [15,17,29,30,48–51].
- [48] D. Stauffer, *Introduction to Percolation Theory* (Taylor & Francis, London, 1985).
- [49] H. Bombin and M. A. Martin-Delgado, Exact topological quantum order in $d = 3$ and beyond: Branyons and brane-net condensates, *Phys. Rev. B* **75**, 075103 (2007).
- [50] E. Knill, Quantum computing with realistically noisy devices, *Nature (London)* **434**, 39 (2005).
- [51] P. Aliferis, D. Gottesman, and J. Preskill, Quantum accuracy threshold for concatenated distance-3 codes, *Quantum Inf. Comput.* **6**, 97 (2006).
- [52] D. A. Lidar and T. A. Brun, edited by *Quantum Error Correction* (Cambridge University Press, Cambridge, England, 2013).
- [53] J. Preskill, in *Introduction to Quantum Computation*, edited by H.-K. Lo, S. Popescu, and T. Spiller (World Scientific, Singapore, 1998).
- [54] D. Gottesman, Stabilizer codes and quantum error correction, Ph.D. thesis, California Institute of Technology, 1997, [arXiv:quant-ph/9705052](https://arxiv.org/abs/quant-ph/9705052).
- [55] H. Mabuchi and P. Zoller, Inversion of Quantum Jumps in Quantum Optical Systems under Continuous Observation, *Phys. Rev. Lett.* **76**, 3108 (1996).
- [56] C. H. Bennett, D. P. DiVincenzo, and J. A. Smolin, Capacities of Quantum Erasure Channels, *Phys. Rev. Lett.* **78**, 3217 (1997).